ACS APPLIED BIO MATERIALS

Article

Inhibition of Fungal Growth using Modified TiO2 with Core@Shell Structure of Ag@CuO Clusters

Maria Guadalupe Mendez Medrano, Ewa Kowalska, Maya Endo Kimura, Kunlei Wang, Bunsho Ohtani, Daniel Bahena Uribe, Jose Luis Rodriguez Lopez, and Hynd Remita

ACS Appl. Bio Mater., **Just Accepted Manuscript** • DOI: 10.1021/acsabm.9b00707 • Publication Date (Web): 21 Oct 2019

is published by the American Chemical Society. 1155 Sixteenth Street N.W., Washington, DC 20036

Graphical abstract

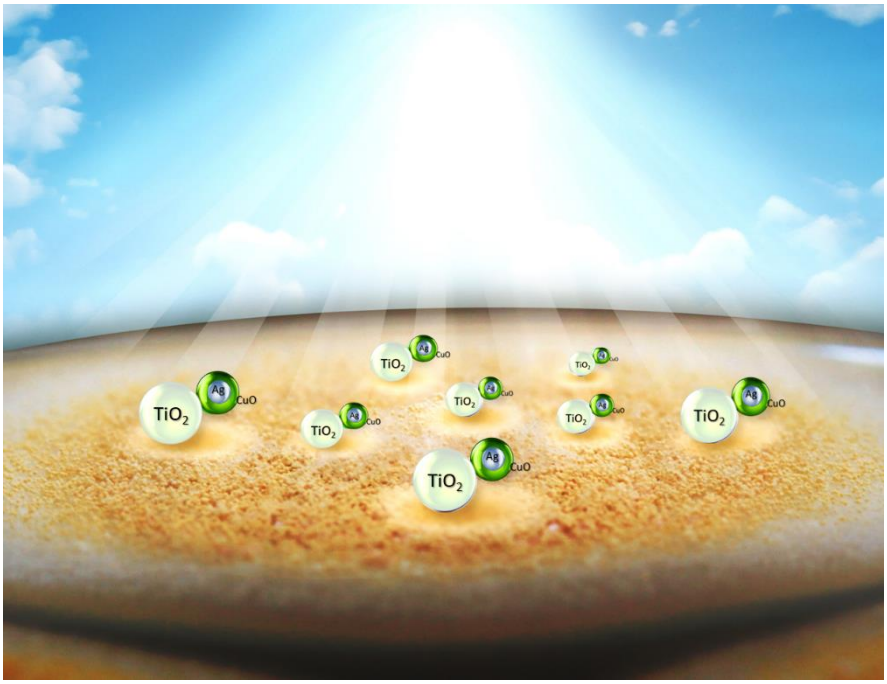

Inhibition of Fungal Growth using Modified TiO_2 with Core@Shell Structure of Ag@CuO Clusters

Maria Guadalupe Méndez-Medrano,[a,b,I] Ewa Kowalska,[c] Maya Endo-Kimura,[c] Kunlei Wang,[c] Bunsho Ohtani,[c] Daniel Bahena Uribe,[d] Jose Luis Rodríguez-López,[b,] and Hynd Remita.[a,e,*]*

[a] Laboratoire de Chimie Physique, UMR 8000 CNRS, Université Paris-Sud, Université Paris-Saclay, 91405 Orsay, France.

[b] Advanced Materials Department, IPICYT, 78216 San Luis Potosi, SLP, Mexico.

[c] Institute for Catalysis, Hokkaido University, Sapporo 001-0021, Japan

[d] Centro de Investigacion y de Estudios Avanzados del Instituto Politecnico Nacional, l07360, D.F., Mexico.

[e] CNRS, Laboratoire de Chimie Physique, UMR 8000, 91405 Orsay, France.

*hynd.remita@u-psud.fr, jlrdz@ipicyt.edu.mx

[I] Present address : Laboratoire de Physique des Interfaces et des Couches Minces, UMR 7647 CNRS, École Polytechnique, 91120 Palaiseau, France.

ABSTRACT

The photocatalytic disinfection (PCD) properties of TiO_2 have attracted the attention in the research communities because the produced reactive oxygen species (ROS) allow destruction of different types of microbes, like fungi, bacteria, viruses, algae, unicellular organisms, etc. on surfaces, in water and air. However, TiO_2 requires UV irradiation to produce the ROS species, which limits its photoactivity in indoor environments. Surface-modified TiO_2 with small Ag and CuO-nanoclusters in core-shell structure exhibits antifungal properties under dark and visible conditions, possibly because of the interaction between Ag-CuO nanoclusters and the fungi membrane and their penetration, and the co-presence of Cu^{2+} and Ag^{+} ions. Therefore, a synergetic effect is obtained with co-modification of TiO_2 with silver and copper and the sample Ag@CuO/TiO_2 (core-shell structure of Ag-Cu at the ratio of 1:3) exhibits the highest antifungal activity, i.e., fungi growth inhibition is observed for *Aspergillus melleus (A. melleus)* and *Penicillium chrysogenum (P. chrysogenum)*. Moreover, significant inhibitions of the sporulation and generation of droplets, possibly containing mycotoxins and sclerotia under dark and visible exposition, are also obtained.

KEYWORDS

Photocatalytic disinfection, TiO_2, Antifungal properties, Ag@CuO, *Aspergillus melleus*, *Penicillium chrysogenum*,

INTRODUCTION

TiO_2 is the most often used material in photocatalysis because of its various features: It is highly photoactive, it is also abundant, cheap and stable. TiO_2 is commonly used and studied for different applications, such as degradation of organic pollutants, hydrogen production,

CO_2 reduction and self-cleaning surfaces (glass, concrete, textile and paints). Also, self-cleaning surfaces have excelled in recent years in environmental fields, and therefore TiO_2 has been frequently used for self-cleaning coatings, due to its photo-induced super-hydrophilicity and photocatalytic activity.[1] TiO_2 presents also the ability to destroy microbes. Most of the studies on the antimicrobial activity of TiO_2 had been performed with the most accessible microorganisms, such as viruses and bacteria.[2,3,4,5,6] Matsunaga *et al*. described in 1985, the photocatalytic activity of TiO_2 for the elimination of *Escherichia coli, Saccharomyces cerevisiae* and *Lactobacillus acidophilus* with possible applications in water and air disinfection.[7] Protozoa algae, and fungi have been shown to be vulnerable to photocatalytic disinfection (PCD), though fungal spores demonstrated more stability inactivation than other vegetative microorganisms.[8] Nevertheless, TiO_2-based photocatalysts can be used in liquid phase or immobilized on surfaces to degrade pollutants found in indoor environment spaces, such as homes, hospitals and offices. It is known that the dusts contain a high number of microorganisms (around 70%), and the principal group of microorganisms presents in bioaerosol are filamentous fungi. They can be a risk to human health, causing respiratory diseases, fungal infections and allergic reactions. Therefore, to face issues with indoor environment quality (IEQ), the fungal contamination must be studied, treated and controlled.[9]

Because of the value of its energy band gap (3.0 eV for rutile and 3.2 eV for anatase), TiO_2 is photoactive only under UV irradiation (which constitutes 4% of the solar spectrum).[10] An indoor environment free of microorganisms is highly desirable to avoid infections in our daily lives. Therefore, intensive studies have been conducted to modify TiO_2 to extend its photoactivity toward the visible range, and thus utilize indoor light sources, without exclude

the use of solar light. The rational design and development of plasmonic photocatalysts, in particular surface modified TiO_2 with plasmonic nanoparticles (NPs), such as Au, Ag and Cu, offers an interesting option.[11,12,13,14,15] The use of chemical compounds or various materials that present antimicrobial and antifungal properties can improve the environmental quality, e.g., in hospitals, where infections are the most common complications, which can even cause the death of patients. Antibacterial effects of TiO_2 can be enhanced by its surface modification with Ag or CuO NPs, which are also well known for their own antibacterial and antifungal properties.[9,16,17,18]

There is evidence that the modification of TiO_2 with Ag or/and CuO NPs might improve the environmental quality under dark and visible light, as a result of: *(i)* the formation of ROS species under visible light attributable to the localized surface plasmon resonance (LSPR) of Ag NPs;[2,8] *(ii)* the narrower bang gap of CuO (1.7 eV),[11,15] and, *(iii)* the TiO_2-based NPs can penetrate inside the microorganism cells, or that the NP_S may attach to the surface of the cell membrane perturbing its permeability and breath functions of the cell;[19] *(iv)* the presence of Ag^+ ions results in protons leakage through the microorganism membrane, reacting with oxygen producing reactive oxygen species $O_2^{\cdot -}$, and this phenomenon causes de-energization of the membrane and consequently cell death,[20] and Cu^{II}-based nanoclusters that lead to the production of Cu^+ ions, which are capable to achieve molecular oxygen reduction.[21,22] These effects play a role in mechanisms' killing in dark and under visible light, affecting the membrane permeability and the cell wall damage, thus resulting in leakage of small molecules, as well as larger molecules, such as proteins, and degeneracy of the inside components of the cells, and ultimately, the cell death.

In this article, the synergetic effect of silver and copper (present in the phase as Ag@CuO NPs, core-shell structure supported on commercial titanium dioxide TiO_2-P25) is presented for the growth inhibition of two different fungi: *(A. melleus)* and *(P. chrysogenum)*.

EXPERIMENTAL

Materials

For the study, TiO_2 powders was supplied from Degussa Evonik P25 (TiO_2-P25). TiO_2-P25 is one of the most active titania photocatalysts, composed the crystalline phases of anatase (73-85 %) and rutile (14-17%), with a small amount of amorphous titania (0-13%).[23] As metal precursors, silver sulfate (Ag_2O_4S, Fulka, ACS reagent ≥ 99.4%) and copper (II) sulfate ($CuSO_4$, Sigma-Aldrich, ReagentPlus®, ≥ 99%) were utilized. 2-propanol ($(CH_3)_2CHOH$, Sigma, 99.5%), malt extract agar (MEA, Merck), NaCl (Wako Pure Chemical Industries, purity ≥ 99.5%) and Milli-Q water at 18.2 MΩ were used. Antifungal tests were performed for two kinds of filamentous fungi, i.e., *(A. melleus)* and *(P. chrysogenum)*, isolated from the air.

Photocatalyst preparation: Surface-modification of TiO_2 with Ag and/or CuO clusters. Aqueous solutions containing 0.1 M of 2-propanol (added to scavenge oxidative $HO^{\bullet}$ radicals ($E^0(HO^{\bullet}/H_2O) = +2.8\ V_{NHE}$) generated by water radiolysis)[24] and metal salts Ag_2SO_4 ($1x10^{-3}$ M), $CuSO_4$ ($1x10^{-3}$ M) or a mixture of the two metal precursors Ag_2SO_4 and $CuSO_4$ (total metal concentration $1x10^{-3}$ M) were added to TiO_2-P25 particles. The suspensions were dispersed by sonication, degassing with nitrogen gas, and then exposed to a panoramic

gamma irradiator ^{60}Co at a dose rate of 4.2 kGy h^{-1} for 3.5 h to insure complete reduction of metal salts. The Ag^+ and/or Cu^{2+} ions can be reduced by solvated electrons ($E^0(H_2O/e^-_s)$ = -2.87 V_{NHE})) and hydroxyl radicals ($E^0((CH_3)_2CO/(CH_3)_2C^{\bullet}OH)$ = -1.8 V_{NHE}), formed by the reaction of $HO^{\bullet}$ (generated by water radiolysis) with 2-propanol.[24] The applied dose is enough to reduce all the metal ions in solution to their zero valency.[15] Three different Ag:Cu molar ratios were used 1:1, 3:1, and 1:3, keeping the total nominal metal content at 1 wt%.

The modified TiO_2−P25 photocatalyst powders were collected after centrifugation and dried at 60°C for 18 h. The supernatants were totally transparent, which indicated that all the Ag^+ and/or Cu^{2+} were reduced and completely deposited on TiO_2−P25.[24,25]

The samples were labeled as, (a) Ag/P25, (b) Ag@CuO1:3/P25, (c) Ag@CuO1:1/P25, (d) Ag@CuO3:1/P25, and (e) CuO/P25 and P25.

Materials Characterization

For High angle annular dark field scanning transmission electron microscopy (HAADF−STEM) analysis, gold-coated holey carbon grid were used as a sample holder, one drop of a suspension (samples in 2-propanol) was dispersed on the grid and dried under N_2 flow. The HAADF−STEM images were acquired with angles of 70−280 mrads and camera length of 8 cm recorded using a Cs corrected JEOL-ARM-200F electron transmission microscope at 200 kV.

Mapping energy dispersive X-ray spectroscopy (EDS) measurements were taken with a detector from Oxford Instruments in solid state with an 80 mm^2 window. X-ray photoelectron spectroscopy (XPS) spectra were obtained by a JEOL JPS-9010MC using Mg Kα radiation, with a hemispherical analyzer. The samples, supported on carbon films, were analyzed with

a pressure < 10^{-7} Torr. Five elements (Ti, O, C, Ag, and Cu) were scanned at high resolution, 50 scans were taken for Ti and O, 300−500 scans for Ag and Cu, and 100 scans for C. Diffuse reflectance spectra (DRS) were registered with a Cary 5000 Series, equipped with an integrating sphere and using KBr as a reference sample.

Antifungal properties for the modified titania with Ag and CuO

The inhibition of fungal growth in the presence of the photocatalysts was examined for *(A. melleus)* and *(P. chrysogenum)* by the agar plate method supplemented with a dispersion of 20 g dm^{-3} of the photocatalysts in 48 g dm^{-3} of MEA (Malt Extract Agar). The suspension was first sterilized in an autoclave at 121°C for 10 min, and then deposited in Petri dishes forming a gel. Ten-day old fungal cultures on MEA slants at 25 °C were used for preparation of spore suspensions. 5 μL of fungal spores were dispersed in 8.5 g/L of NaCl solution contained in a slant. The slant was then vigorously shaken by a Vortex for 3 min. Three drops of 5 μL of fungal spores were inoculated on Petri plates and incubated at room temperature under natural indoor light (intensity of ca. 120 Wm^{-2}) and in the dark. The incubation was carried out for 8 days at 25 °C. The colony diameters were measured after 2, 4, 6, and 8 days of incubation. The daily growth rates has been estimated by fitting the linear regression equation:

$$r = at + b \qquad (1)$$

In which r - colony radius (mm); a - daily growth rate; t - incubation time (days), and b - growth retardation time (lag phase; λ). This activity was analyzed, as well as the appearance (color, the droplets) of mycelium.

Results and discussion

The modified TiO_2 samples were characterized by HAADF−STEM, and the observations showed nanoclusters supported on TiO_2-P25 surface for Cu/P25 and Ag/P25 samples. These clusters are smaller in size (between 1-2 nm) than the nanoparticles obtained with co-modification with Ag and Cu, where bigger nanoparticles in size around 5−12 nm were found, as is shown in Figure 1A. The EDS analysis, represented by elemental mapping composition for co-modified TiO_2), is described in Figure 1B. The maps show NPs in a core(Ag)-shell(Cu-based) structure. TiO_2 is surface-modified with Ag nanoparticles surrounded by Cu-based nanoclusters. The contrast of the core-shell metal nanoparticles on TiO_2 indicates that its core of the metal nanoparticles increases in size with Ag loading.

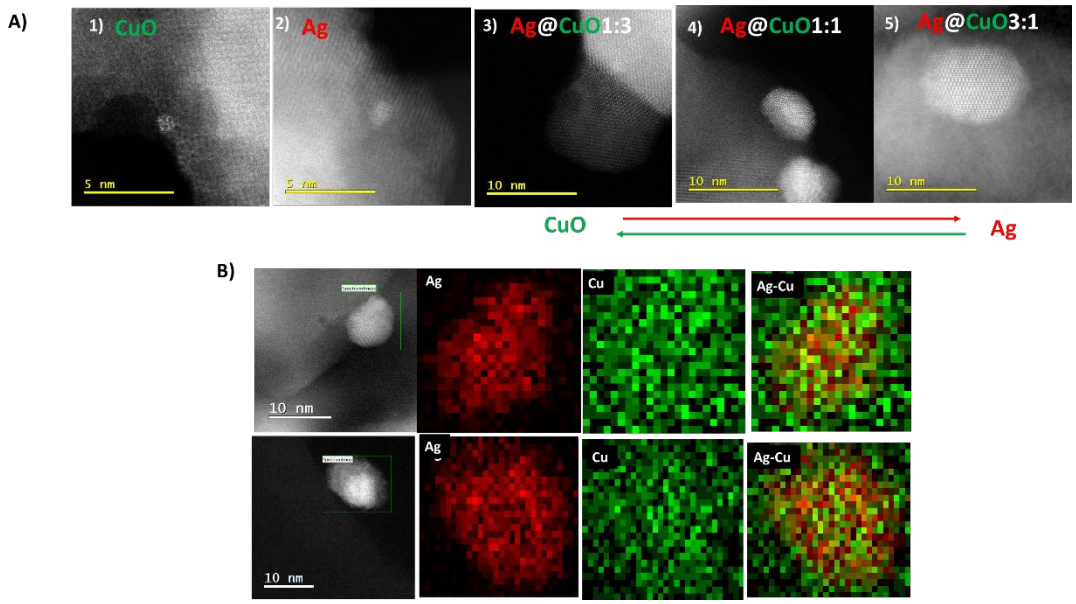

Figure 1. A) HAADF-STEM images of 1) CuO/P25, 2) Ag/P25, 3)Ag@CuO1:3/P25, 4) Ag@CuO1:1/P25, and 5) Ag@CuO3:1/P25. (B) Chemical mapping performed on nanoparticles of Ag@CuO1:1/P25 (Ag and Cu in red and green spots, respectively).

The modified TiO_2 samples were analyzed by XPS, as provided in Figure S1. The peaks Ti $2p_{3/2}$ at 459.5 eV and Ti $2p_{1/2}$ at 465.5 eV are the orbitals characteristic of Ti^{4+} in TiO_2 and the peak at 530.5 eV is attributed to oxygen 1s orbital of TiO_2. In Figure S2a, metallic Ag was represented by the position of the two reproducible components, Ag $3d_{5/2}$ at 368.3 eV and Ag $3d_{3/2}$ at 374.3 eV, and their separation ($\Delta_{BE}(Ag3d_{5/2-3/2})$ = 6.0 eV).[11,26,27,28,29] The additional, smaller peaks at higher binding energies localized at 368.6 eV and 374.5 eV respectively, correspond to the interaction of Ag NPs with titania as it has been previously reported.[11, 28,29,30]

In the Figure S2b, Cu core peaks are observed (Cu $2p_{1/2}$ and Cu $2p_{3/2}$)[31,32] at binding energies localized in the range of 953.3 − 953.5 eV and 933.3 − 933.6 eV respectively. These values had been related to Cu^{II},[31,33] however the characteristic shake-up of Cu^{II} is not present. It has been reported by Chusue *et al.* that this satellite can be modified or even disappear, depending of the particle size Cu^{II}, and on the reduction state of Cu.[34]

The DRS spectra are shown in the Figure 2. The TiO_2−P25 spectrum exhibits an absorption at around 400 nm, which is mainly related to rutile (narrower bandgap than that by anatase).[35] All the modified samples with Ag NPs and CuO nanoclusters present a small shift to higher wavelengths. This effect has been reported as the equilibrium between the conduction band (CB) of TiO_2-P25 by its junction with nanoparticles (Ag NPs and CuO nanoclusters).[15] The samples with different ratios of Ag@CuO, exhibit absorptions bands with maxima at 510 nm and 800 nm. The absorption at 510 nm is related to the LSPR of Ag NPs, being red-shifted. This red-shift of LSPR is typically seen and reported as an effect of the interaction of the metal NPs with the TiO_2 support, showing a high reflective index.[11,12,15,36] It is well known that the LSPR position change is dependent of the surrounding medium and the support.[37]

The broad absorption band with a maximum at 800 nm is due to CuO nanoclusters. The modification of titania with CuO clusters induces the extension of its absorption to the visible range of the solar spectrum. The absorption band of CuO/P25 in the near IR is due to the $2Eg \rightarrow 2T2g$ inter-band transitions of Cu^{II}-based clusters deposited on different phases and sites of titania and with strong interaction with it.[33]

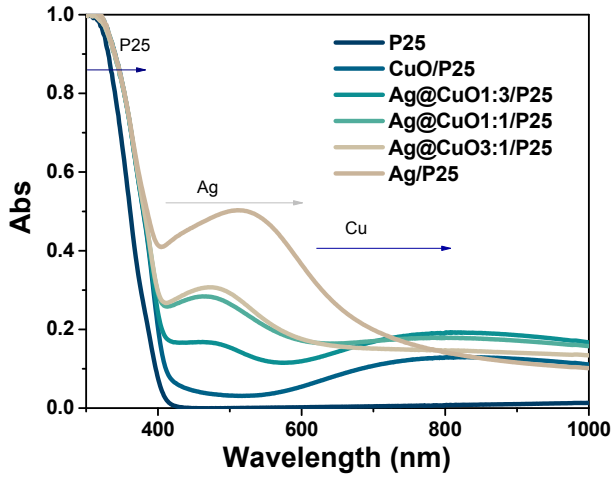

Figure 2. Optical DRS spectra of P25, CuO/P25, Ag@CuO1:3/P25, Ag@CuO1:1/P25, Ag@CuO3:1/P25 and Ag/P25, showing the regions of the plasmon band of Ag and the absorption band of CuO.

The photocatalysts exhibit different colors, as shown in Figure 3: light green for TiO_2 modified with copper, purple for titania modified with silver and light-brown or creamy with co-modifications.

Figure 3. Pictures of the modified TiO_2 with Ag, CuO and Ag@CuO clusters (with different Ag/Cu ratios).

The antifungal activities were studied for mycelium (vegetative part of a fungus, consisting of a mass of branching, thread-like filamentous structure of a fungus) growth under dark and visible light illumination. Two fungi were used: *(A. melleus)* and *(P. chrysogenum)*. The rate of fungal daily growth was evaluated in dark and under visible light irradiation, in media composed of pure and modified TiO_2 (with Ag, CuO and Ag@CuO NPs).

Figure 4 and Figure S3 show the fungal daily growth for *(A. melleus)* and *(P. chrysogenum)* in a control media (no titania), as well as with pure and modified titania samples. The mycelium grew faster in the dark than under visible light irradiation in a control media (without titania) for both species. In the presence of TiO_2-P25, the growth of *(A. melleus)* was significantly decreased under visible irradiation. Although, titania is inactive under vis irradiation, the presence of rutile with narrower bandgap than that of anatase might result in its slight vis response, as already reported by Markowska-Szczupak et al.[2] It has been reported that the absorption of more photons (narrower bandgap) might be the reason of

higher activity of rutile (separated from P25) than that of anatase (also obtained from P25) for the methanol dehydrogenation under UV/vis irradiation. Moreover, it should be pointed that natural indoor light was used for this study, containing also UV part, and thus both polymorphs might be excited. However, *(P. chrysogenum)* shows the opposite behavior: An acceleration of the fungus growth under visible light irradiation. It has been reported that anatase phase can stimulate the fungal growth because of its superhydrophilic properties, which can change with irradiation.[2] In the dark, both fungi present a decrease of growth, and according to Calvo *et al.,* the inhibition of fungal growth can be due to titania adsorption on fungal surface, which can decrease the sporulation.[38]

Regarding co-modifications with Ag and CuO, for *(A. melleus),* it should be pointed out that the presence of Ag NPs (Ag/P25 and Ag@CuO3:1/P25) accelerated the growth in the dark, and the presence of CuO nanoclusters (CuO/P25, Ag@CuO1:3/P25 and Ag@CuO1:1/P25) decreases the growth under visible light irradiation. In contrast, for *(P. chrysogenum)*, an acceleration of the growth of the fungi is observed under visible irradiation in the presence of Ag NPs, with the exception of the sample Ag@CuO1:3/P25. In dark, all the modified samples show an inhibition in the growth, with the exception of CuO/P25.

Therefore, a synergistic effect is obtained with co-modification of $TiO_2$with silver and copper oxide: The system Ag@CuO/P25 with the ratio1:3 presents the highest antifungal activity for both fungi under both dark and visible conditions (see Fig. 4).

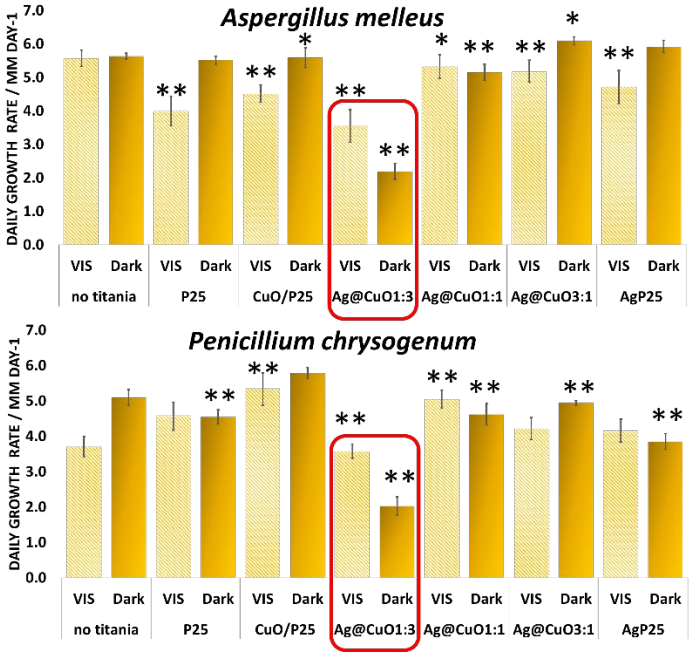

Figure 4. Daily growth of fungi after 8 days of incubation, under visible (vis) and in dark for *(A. melleus)* (up) and *(P. chrysogenum)* (bottom), accompanied by its statistical analysis significance compared with no titania on visible and dark fungal growth. **p* (italic) < 0.05 and ***p* < 0.01.

The changes of the mycelium diameters and the color of the spores in the media, with bare and modified (with Ag@CuO1:3) TiO_2-P25 are shown in the Figure 5 and Figure S4.

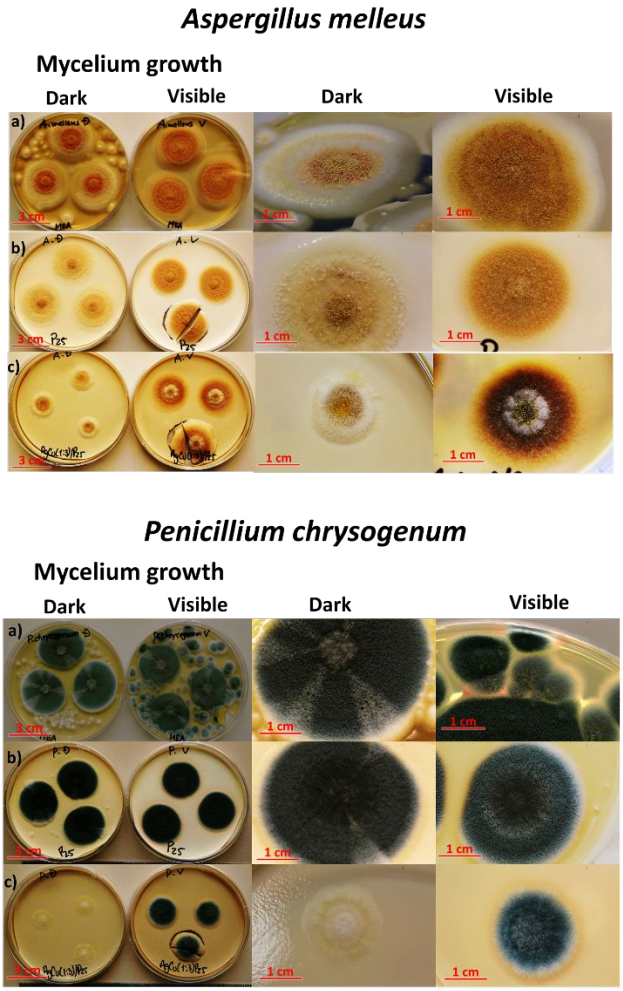

Figure 5. Photographs of mycelium growth of *(A. melleus)* (up) and *(P. chrysogenum)* (bottom) fungi after 8 days incubation of a) blank (no titania), b) TiO_2-P25, and c) Ag@CuO1:3/P25 under visible light and in dark. The left pictures: pictures at the scale of the fungi growth, and the right pictures: the extension of a mycelium.

Moreover, significant inhibition of the sporulation and droplets, possibly containing mycotoxins and sclerotia (pink spheres structures in the case of *(A. melleus)*) for the sample Ag@CuO1:3 in dark and under visible light exposition was observed, as it can be seen in Figure 6. One can see clearly the reduction of the number of spores and the decrease of their

diameters, which is essential for the prevention against the toxic effect of mycotoxins in humans and animals. Mycotoxin production is associated to sporulation.[38]

A slight decrease of the sporulation and possible mycotoxin generation is also observed for TiO_2-P25, as shown in the Figure 5. However, for titania modified with Ag@CuO1:3, mycotoxins have not been detected at all, and significant inhibition of sporulation has been observed.

For *(P. chrysogenum)*, observed droplets with possibly containing mycotoxins, are only present in the blank sample, i.e., on the media. The presence of TiO_2-P25 inhibits the formation of droplets under dark and visible light. In the case of Ag@CuO3:1/P25, inhibition of the sporulation and possible mycotoxin formation is observed after 8 days of exposition under visible light, but mostly in the dark.

Different behaviors in the inhibition of fungal growth were observed for *(A. melleus)* and *(P. chrysogenum)*. Indeed, Markowska-Szczupak *et al*. reported that the antifungal activity of TiO_2-P25 depends considerably on the nature of the fungi.[2] However, the best growth inhibition for both fungi under dark and visible light exposition was obtained for the sample Ag@CuO1:3/P25 showing a synergistic effect of Ag and CuO NPs.

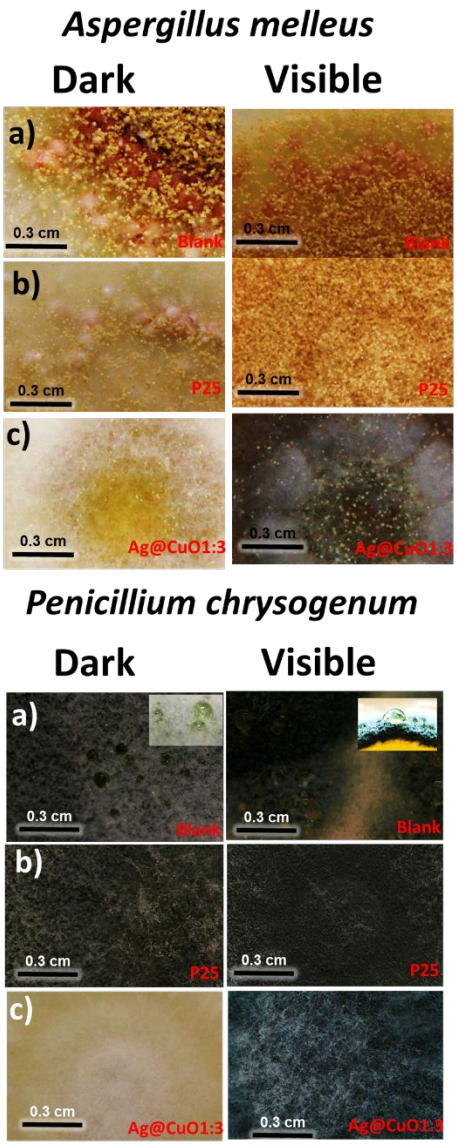

Figure 6. Picture of 8-day growth of (A. melleus) and (P. chrysogenum) in the dark and under visible exposition. a) Under media (blank), b) with pure TiO_2-P25, and c) with TiO_2-P25 surface-modified with Ag@CuO1:3.

Our results show the high antifungal activity of TiO_2 co-modified with CuO@Ag NPs (with a Ag/Cu ratio of 1:3), and a mechanism is proposed in Figure 7. Under visible light irradiation, CuO nanoclusters (band gap 1.7 eV) and plasmonic Ag NPs inject electrons in

the CB of TiO_2[15]. Thus, ROS species are generated: the excited electrons reduce the atmospheric oxygen forming oxidative $O_2^{-\cdot}$ radicals, while the generated holes can generate oxidative $HO^{\bullet}$ radicals (reactive with water) and/or oxidize directly organic molecules. Interestingly, much higher activity in the dark than that under visible light was observed for the sample Ag@CuO1:3/P25. It was reported by Qiu et al.[22] that few-nanometer size of the CuO clusters could be critical for high antibacterial activity. It was proposed that the Cu^{2+} ions led to the formation of Cu^{+} species with strong anti-pathogenic (antibacterial and anti-viral activities) effects, even under dark conditions.[21,39,40] It is also well known that Ag NPs exhibit antibacterial activity even in the dark.[20] Ag^{+} ions highly react with the present –SH groups on biomolecules to inactivate the bacteria, and the antibacterial activities depend on the chemisorbed metal ions (surface oxidation), and also the size of Ag NPs plays a role, i.e., small Ag NPs with higher surface area available for the interaction with the membrane, exhibit higher activity than larger particles. Moreover, Ag NPs might adhere at the cell membrane impeding the breathing function of the cell and its permeability. Another possibility is that Ag NPs can also cross the membranes and penetrate inside the microorganisms.[20,41,19,42]

The most interesting finding is the difference between the activity under the dark and visible light exposition especially for the most active sample Ag@CuO1:3/P25. Although activity enhancement under visible light irradiation could be simply explained by enhanced light harvesting by the two modifiers, the reason of much higher activity in the dark for both fungi is unknown and could be only speculated. For example, under visible irradiation positively charged plasmonic silver NPs (after transfer of hot electrons from Ag NPs to the CB of TiO_2-P25)[15] could be a desirable form for antifungal properties (along to well-known

antibacterial properties of Ag^+). Higher inhibition of fungal growth under visible irradiation than that in the dark on Ag/P25 for *(A. melleus)* supports this hypothesis.

For the samples co-modified with silver and copper, under visible irradiation "hot" electrons from silver NPs migrate rather to CuO instead to TiO_2, as shown by previous TRMC (time resolved microwave conductivity) experiments,[15] resulting in reduction of Cu(II) to Cu(I), and thus in a decrease in activity of CuO.

Moreover, higher antifungal activity of CuO/P25 under visible light exposition than that in the dark for both fungi, and at the same slightly lower than that of pure TiO_2-P25 (especially for *(P. chrysogenum)*) strongly suggests us that some synergy between both modifiers is responsible for enhanced antifungal properties. It is proposed that fine CuO nanoclusters adsorbed on silver nanoparticles accelerate the attachment of the NPs to fungal cells. The strongest enhancement of antifungal properties is observed for Ag to CuO molar ratio of 1:3, where higher content of small CuO clusters, concentrated on smaller Ag cores are present in comparison to other co-modified samples, as observed by HAADF-STEM (Figure 1). Titania modified with Ag@CuO at molar ratio of 1:3 provides small Ag and Cu-based particles, which not only interact with the membrane of the fungi, but can also penetrate inside the membranes increasing more efficiently the inhibition of fungi growth. These small nanoparticles have higher surface area because of their size, and therefore Ag cores are more easily oxidized leading to Ag^+ ions leaching as well as Cu^{2+} ions release, and therefore these metal ions can also be responsible of the fungi growth inhibition, as is presented in Figure 7a. Under visible light exposition (Figure 7b), excited CuO NPs can reduce Ag^+ ions to Ag^0 and, because of Ag surface localized plasmon resonance, hot electrons can reduce Cu^{II} into Cu^{I}, and this can explain the decrease of the activity under visible irradiation.

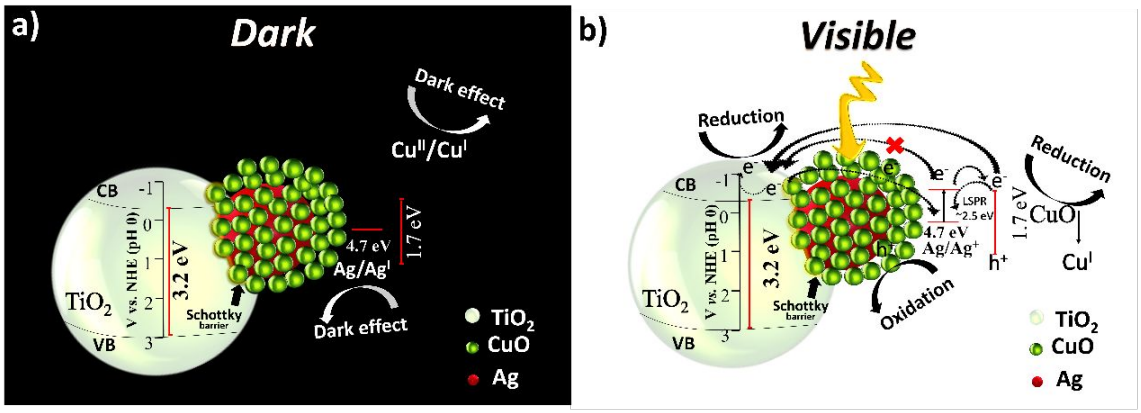

Figure 7. Mechanism proposed for photocatalytic inactivation of *(A. melleus)* and *(P. chrysogenum)* fungi for Ag@CuO core-shell NPs on TiO_2 in a) the dark and under b) visible light irradiation.

CONCLUSION

Nanoparticles of CuO, Ag and Ag@CuO supported on the surface of TiO_2-P25 were synthesized by radiolysis. HAADF-STEM and XPS characterizations showed that, in the case of co-modification with silver and copper, core-shell nanoparticles composed of silver core and CuO shell (in the form of small clusters) were obtained on titania. A synergistic effect of anti-fungal activity for *A. melleus* and *P. chrysogenum* was obtained in the dark and under visible light exposition for titania co-modified with Ag and CuO, which was observed as inhibition of fungal growth, and the lack of possible mycotoxin formation. The highest antifungal properties were obtained with the sample Ag@CuO1:3/P25, in the dark and under visible light irradiation. These colored photocatalysts can be applied for self-cleaning surfaces with anti-microbial and antifungal activities in the dark and under visible light irradiation, in hospitals, pharmaceutical industries, food industries etc., improving the indoor environment quality.

ASSOCIATED CONTENT

†Electronic Supplementary Information (ESI) available: Additional information of binding energies by XPS analysis, diameter of fungi growth and the photographs of mycelium growth.

AUTHOR INFORMATION

Corresponding Author

*hynd.remita@u-psud.fr; Tel: +33 (0)1 69 15 72 58.

*jlrdz@ipicyt.edu.mx; Tel : +52 444 834 2000 x 7217

Present address:

M.G. Méndez-Medrano : Laboratoire de Physique des Interfaces et des Couches Minces, UMR 7647 CNRS, École Polytechnique, 91120 Palaiseau, France.

Author Contributions

M.G. Méndez-Medrano synthesized and characterized the materials, performed the antifungi tests and wrote the manuscript, M. Endo-Kimura and K. Wang performed the antifungi tests and contributed to their interpretation, D. Bahena characterized the nanomaterials by HAADF-EDS, E. Kowalska and B. Ohtani discussed the results and contributed to the manuscript writing, J.L. Rodríguez-López, and H. Remita conducted the project and contributed to the article writing. The manuscript was written through contributions of all authors. All authors have given approval to the final version of the manuscript.

ACKNOWLEDGMENT

Financial support from the CNRS, ECOS-Nord M11-P02 project (CNRS-CONACYT bilateral project), the CONCERT-Japan Joint Call on Efficient Energy Storage (European Commission), the COST Nanoalloys and CONACYT (Mexico grant numbers 216315 and 356872) are highly acknowledged. M.G.M.M. acknowledges Campus France for the *Eiffel Excellence* Scholarship. The authors acknowledge also C'Nano *Ile de France for* the financial support for *the gamma source*.

REFERENCES

(1) Schaming, D.; Remita, H. Nanotechnology: From the Ancient Time to Nowadays. *Found. Chem.* **2015**, *17*, 187–205.

(2) Markowska-Szczupak, A.; Wang, K.; Rokicka, P.; Endo, M.; Wei, Z.; Ohtani, B.; Morawski, A. W.; Kowalska, E. The Effect of Anatase and Rutile Crystallites Isolated from Titania P25 Photocatalyst on Growth of Selected Mould Fungi. *J. Photochem. Photobiol. B* **2015**, *151*, 54–62.

(3) Guillard, C.; Bui, T.-H.; Felix, C.; Moules, V.; Lina, B.; Lejeune, P. Microbiological Disinfection of Water and Air by Photocatalysis. *Comptes Rendus Chim.* **2008**, *11*, 107–113.

(4) Zhao, J.; Yang, X. Photocatalytic Oxidation for Indoor Air Purification: A Literature Review. *Build. Environ.* **2003**, *38*, 645–654.

(5) Rodriguez, C.; Di Cara, A.; Renaud, F. N. R.; Freney, J.; Horvais, N.; Borel, R.; Puzenat, E.; Guillard, C. Antibacterial Effects of Photocatalytic Textiles for Footwear Application. *Catal. Today* **2014**, *230*, 41–46.

(6) Helali, S.; Polo-López, M. I.; Fernández-Ibáñez, P.; Ohtani, B.; Amano, F.; Malato, S.; Guillard, C. Solar Photocatalysis: A Green Technology for E. Coli Contaminated Water Disinfection. Effect of Concentration and Different Types of Suspended Catalyst. *J. Photochem. Photobiol. Chem.* **2014**, *276*, 31–40.

(7) Matsunaga, T.; Tomoda, R.; Nakajima, T.; Wake, H. Photoelectrochemical Sterilization of Microbial Cells by Semiconductor Powders. *FEMS Microbiol. Lett.* **1985**, *29*, 211–214.

(8) Foster, H. A.; Ditta, I. B.; Varghese, S.; Steele, A. Photocatalytic Disinfection Using Titanium Dioxide: Spectrum and Mechanism of Antimicrobial Activity. *Appl. Microbiol. Biotechnol.* **2011**, *90* (6), 1847–1868.

(9) Kowalska, E.; Wei, Z.; Karabiyik, B.; Herissan, A.; Janczarek, M.; Endo, M.; Markowska-Szczupak, A.; Remita, H.; Ohtani, B. Silver-Modified Titania with Enhanced Photocatalytic and Antimicrobial Properties under UV and Visible Light Irradiation. *Catal. Today* **2015**, *252*, 136–142.

(10) Wang, G.; Xu, L.; Zhang, J.; Yin, T.; Han, D.; Wang, G.; Xu, L.; Zhang, J.; Yin, T.; Han, D. Enhanced Photocatalytic Activity of Powders (P25) via Calcination Treatment. *Int. J. Photoenergy Int. J. Photoenergy* **2012**, *2012*, 265760.

(11) Grabowska, E.; Zaleska, A.; Sorgues, S.; Kunst, M.; Etcheberry, A.; Colbeau-Justin, C.; Remita, H. Modification of Titanium(IV) Dioxide with Small Silver Nanoparticles: Application in Photocatalysis. *J. Phys. Chem. C* **2013**, *117*, 1955–1962.

(12) Linic, S.; Christopher, P.; Ingram, D. B. Plasmonic-Metal Nanostructures for Efficient Conversion of Solar to Chemical Energy. *Nat. Mater.* **2011**, *10*, 911–921.

(13) Kowalska, E.; Mahaney, O. O. P.; Abe, R.; Ohtani, B. Visible-Light-Induced Photocatalysis through Surface Plasmon Excitation of Gold on Titania Surfaces. *Phys. Chem. Chem. Phys.* **2010**, *12*, 2344–2355.

(14) Méndez-Medrano, M. G.; Kowalska, E.; Lehoux, A.; Herissan, A.; Ohtani, B.; Rau, S.; Colbeau-Justin, C.; Rodríguez-López, J. L.; Remita, H. Surface Modification of TiO_2 with Au Nanoclusters for Efficient Water Treatment and Hydrogen Generation under Visible Light. *J. Phys. Chem. C* **2016**, *120*, 25010–25022.

(15) Méndez-Medrano, M. G.; Kowalska, E.; Lehoux, A.; Herissan, A.; Ohtani, B.; Bahena, D.; Briois, V.; Colbeau-Justin, C.; Rodríguez-López, J. L.; Remita, H. Surface Modification of TiO_2 with Ag Nanoparticles and CuO Nanoclusters for Application in Photocatalysis. *J. Phys. Chem. C* **2016**, *120*, 5143–5154.

(16) Yao, X.; Zhang, X.; Wu, H.; Tian, L.; Ma, Y.; Tang, B. Microstructure and Antibacterial Properties of Cu-Doped TiO_2 Coating on Titanium by Micro-Arc Oxidation. *Appl. Surf. Sci.* **2014**, *292*, 944–947.

(17) Chwalibog, A.; Sawosz, E.; Hotowy, A.; Szeliga, J.; Mitura, S.; Mitura, K.; Grodzik, M.; Orlowski, P.; Sokolowska, A. Visualization of Interaction between Inorganic

Nanoparticles and Bacteria or Fungi. *International Journal of Nanomedicine*. 5th ed. 2010, pp 1085–1094.

(18) Janczarek, M.; Endo, M.; Zhang, D.; Wang, K.; Kowalska, E. Enhanced Photocatalytic and Antimicrobial Performance of Cuprous Oxide/Titania: The Effect of Titania Matrix. *Materials* **2018**, *11*, 2069.

(19) Kvítek, L.; Panáček, A.; Soukupová, J.; Kolář, M.; Večeřová, R.; Prucek, R.; Holecová, M.; Zbořil, R. Effect of Surfactants and Polymers on Stability and Antibacterial Activity of Silver Nanoparticles (NPs). *J. Phys. Chem. C* **2008**, *112* (15), 5825–5834.

(20) Sharma, V. K.; Yngard, R. A.; Lin, Y. Silver Nanoparticles: Green Synthesis and Their Antimicrobial Activities. *Adv. Colloid Interface Sci.* **2009**, *145*, 83–96.

(21) Liu, M.; Sunada, K.; Hashimoto, K.; Miyauchi, M. Visible-Light Sensitive Cu(II)–TiO_2 with Sustained Anti-Viral Activity for Efficient Indoor Environmental Remediation. *J. Mater. Chem. A* **2015**, *3* (33), 17312–17319.

(22) Qiu, X.; Miyauchi, M.; Sunada, K.; Minoshima, M.; Liu, M.; Lu, Y.; Li, D.; Shimodaira, Y.; Hosogi, Y.; Kuroda, Y. Hybrid Cu_xO/TiO_2 Nanocomposites as Risk-Reduction Materials in Indoor Environments. *ACS Nano* **2012**, *6* (2), 1609–1618.

(23) Ohtani, B.; Prieto-Mahaney, O. O.; Li, D.; Abe, R. What Is Degussa (Evonik) P25? Crystalline Composition Analysis, Reconstruction from Isolated Pure Particles and Photocatalytic Activity Test. *J. Photochem. Photobiol. Chem.* **2010**, *216*, 179–182.

(24) Remita, H.; Remita, S. Metal Clusters and Nanomaterials: Contribution of Radiation Chemistry. In *Recent Trends in Radiation Chemistry*; World Scientific, 2010; pp 347–383.

(25) Belloni, J.; Mostafavi, M.; Remita, H.; Marignier, J.-L.; Delcourt, and M.-O. Radiation-Induced Synthesis of Mono- and Multi-Metallic Clusters and Nanocolloids. *New J. Chem.* **1998**, *22*, 1239–1255.

(26) Verbruggen, S. W.; Keulemans, M.; Filippousi, M.; Flahaut, D.; Van Tendeloo, G.; Lacombe, S.; Martens, J. A.; Lenaerts, S. Plasmonic Gold–Silver Alloy on TiO_2 Photocatalysts with Tunable Visible Light Activity. *Appl. Catal. B Environ.* **2014**, *156*, 116–121.

(27) Stathatos, E.; Lianos, P.; Falaras, P.; Siokou, A. Photocatalytically Deposited Silver Nanoparticles on Mesoporous TiO_2 Films. *Langmuir* **2000**, *16*, 2398–2400.

(28) Waterhouse, G. I. N.; Bowmaker, G. A.; Metson, J. B. Oxidation of a Polycrystalline Silver Foil by Reaction with Ozone. *Appl. Surf. Sci.* **2001**, *183*, 191–204.

(29) Bielmann, M.; Schwaller, P.; Ruffieux, P.; Gröning, O.; Schlapbach, L.; Gröning, P. AgO Investigated by Photoelectron Spectroscopy: Evidence for Mixed Valence. *Phys. Rev. B* **2002**, *65*, 235431.

(30) Han, Y.; Lupitskyy, R.; Chou, T.-M.; Stafford, C. M.; Du, H.; Sukhishvili, S. Effect of Oxidation on Surface-Enhanced Raman Scattering Activity of Silver Nanoparticles: A Quantitative Correlation. *Anal. Chem.* **2011**, *83*, 5873–5880.

(31) Espinós, J. P.; Morales, J.; Barranco, A.; Caballero, A.; Holgado, J. P.; González-Elipe, A. R. Interface Effects for Cu, CuO, and Cu_2O Deposited on SiO_2 and ZrO_2. XPS Determination of the Valence State of Copper in Cu/SiO_2 and Cu/ZrO_2 Catalysts. *J. Phys. Chem. B* **2002**, *106*, 6921–6929.

(32) Pauly, N.; Tougaard, S.; Yubero, F. Determination of the Cu 2p Primary Excitation Spectra for Cu, Cu_2O and CuO. *Surf. Sci.* **2014**, *620*, 17–22.

(33) Colón, G.; Maicu, M.; Hidalgo, M. C.; Navío, J. A. Cu-Doped TiO_2 Systems with Improved Photocatalytic Activity. *Appl. Catal. B Environ.* **2006**, *67*, 41–51.

(34) Chusuei, C. C.; Brookshier, M. A.; Goodman, D. W. Correlation of Relative X-Ray Photoelectron Spectroscopy Shake-up Intensity with CuO Particle Size. *Langmuir* **1999**, *15*, 2806–2808.

(35) Chiarello, G. L.; Selli, E.; Forni, L. Photocatalytic Hydrogen Production over Flame Spray Pyrolysis-Synthesised TiO_2 and Au/TiO_2. *Appl. Catal. B Environ.* **2008**, *84*, 332–339.

(36) Hai, Z.; Kolli, N. E.; Uribe, D. B.; Beaunier, P.; José-Yacaman, M.; Vigneron, J.; Etcheberry, A.; Sorgues, S.; Colbeau-Justin, C.; Chen, J. Modification of TiO_2 by Bimetallic Au–Cu Nanoparticles for Wastewater Treatment. *J. Mater. Chem. A* **2013**, *1*, 10829–10835.

(37) Mizeikis, V.; Kowalska, E.; Juodkazis, S. Resonant Localization, Enhancement, and Polarization of Optical Fields in Nano-Scale Interface Regions for Photo-Catalytic Applications. *J. Nanosci. Nanotechnol.* **2011**, *11*, 2814–2822.

(38) Calvo, A. M.; Wilson, R. A.; Bok, J. W.; Keller, N. P. Relationship between Secondary Metabolism and Fungal Development. *Microbiol. Mol. Biol. Rev. MMBR* **2002**, *66*, 447–459.

(39) Qiu, X.; Miyauchi, M.; Yu, H.; Irie, H.; Hashimoto, K. Visible-Light-Driven Cu(II)-(Sr(1-y)Na(y))(Ti(1-x)Mo(x))O3 Photocatalysts Based on Conduction Band Control and Surface Ion Modification. *J. Am. Chem. Soc.* **2010**, *132*, 15259–15267.

(40) Chung, C.-J.; Lin, H.-I.; Chou, C.-M.; Hsieh, P.-Y.; Hsiao, C.-H.; Shi, Z.-Y.; He, J.-L. Inactivation of Staphylococcus Aureus and Escherichia Coli under Various Light Sources on Photocatalytic Titanium Dioxide Thin Film. *Surf. Coat. Technol.* **2009**, *203* (8), 1081–1085.

(41) Wei, Z.; Endo, M.; Wang, K.; Charbit, E.; Markowska-Szczupak, A.; Ohtani, B.; Kowalska, E. Noble Metal-Modified Octahedral Anatase Titania Particles with Enhanced Activity for Decomposition of Chemical and Microbiological Pollutants. *Chem. Eng. J.* **2016**.

(42) Morones, J. R.; Elechiguerra, J. L.; Camacho, A.; Holt, K.; Kouri, J. B.; Ramírez, J. T.; Yacaman, M. J. The Bactericidal Effect of Silver Nanoparticles. *Nanotechnology* **2005**, *16*, 2346–2353.

Graphical abstract

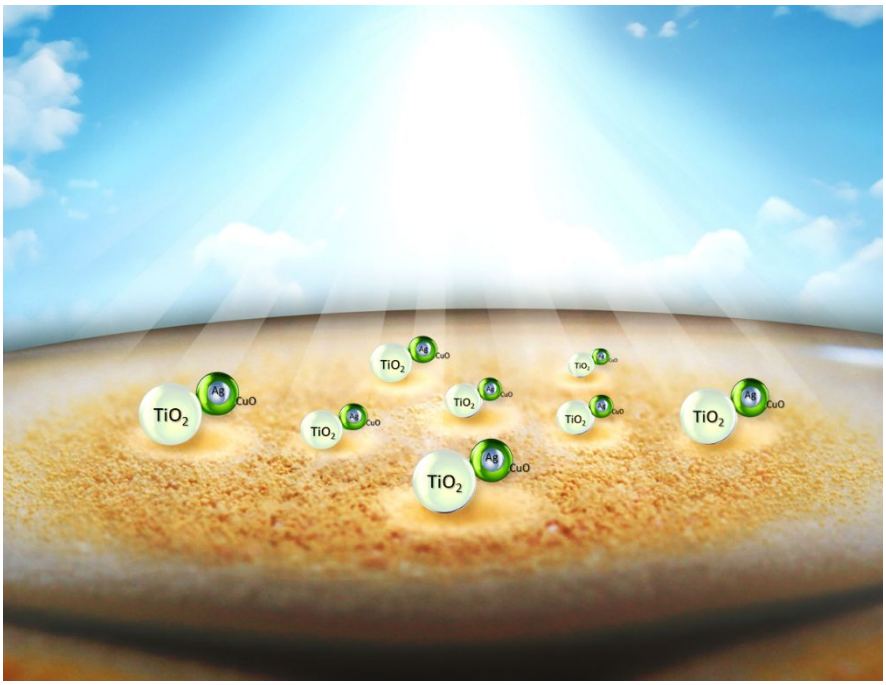
TiO2
CuO
TiO2
CuO
TiO2
CuO
TiO2
CuO
TiO2
CuO
TiO2
CuO
TiO2
CuO